

Pilot trial of sunitinib therapy in patients with von Hippel–Lindau disease

E. Jonasch^{1*}, I. E. McCutcheon², S. G. Waguespack³, S. Wen⁴, D. W. Davis⁵, L. A. Smith¹, N. M. Tannir¹, D. S. Gombos⁶, G. N. Fuller⁷ & S. F. Matin⁸

Departments of ¹Genitourinary Medical Oncology; ²Neurosurgery; ³Endocrine Neoplasia and Hormonal Disorders; ⁴Biostatistics, The University of Texas M. D. Anderson Cancer Center, Houston; ⁵ApoCell, Inc, Houston; Departments of ⁶Ophthalmology; ⁷Pathology; ⁸Urology, The University of Texas M. D. Anderson Cancer Center, Houston, USA

Received 23 September 2010; revised 13 December 2010; accepted 3 January 2011

Background: Von Hippel–Lindau (VHL) disease induces vascular neoplasms in multiple organs. We evaluated the safety and efficacy of sunitinib in VHL patients and examined the expression of candidate receptors in archived tissue.

Methods: Patients with VHL were given four cycles of 50 mg sunitinib daily for 28 days, followed by 14 days off. Primary end point was toxicity. Modified RECIST were used for efficacy assessment. We evaluated 20 archival renal cell carcinomas (RCCs) and 20 hemangioblastomas (HBs) for biomarker expression levels using laser-scanning cytometry (LSC).

Results: Fifteen patients were treated. Grade 3 toxicity included fatigue in five patients. Dose reductions were needed in 10 patients. Eighteen RCC and 21 HB lesions were evaluable. Six of the RCCs (33%) responded partially, versus none of the HBs ($P = 0.014$). LSC revealed that mean levels of phosphorylated vascular endothelial growth factor receptor-2 were lower in HB than in RCC endothelium ($P = 0.003$) and mean phosphorylated fibroblast growth factor receptor substrate-2 (pFRS2) levels were higher in HB ($P = 0.003$).

Conclusions: Sunitinib treatment in VHL patients showed acceptable toxicity. Significant response was observed in RCC but not in HB. Greater expression of pFRS2 in HB tissue than in RCC raises the hypothesis that treatment with fibroblast growth factor pathway-blocking agents may benefit patients with HB.

Key words: endothelium, hemangioblastoma, renal cell carcinoma, sunitinib, VHL

Introduction

Von Hippel–Lindau disease (VHL) is an autosomal dominant inherited disease occurring in approximately one in 35 000 births [1]. VHL is characterized by the development of retinal and central nervous system (CNS) hemangioblastomas (HBs), pheochromocytomas, pancreatic cysts and cystadenomas, pancreatic neuroendocrine tumors (NETs), renal cysts, and clear-cell renal cell carcinomas (RCCs) [1]. Before regular screening of patients with VHL began, their median survival time was ~50 years [2, 3]. Morbidity and mortality of these individuals arises primarily from neurologic compromise owing to HB and RCC progression. Improving our ability to modulate RCC and CNS progression will clearly affect the morbidity and mortality of VHL.

A concerted effort to elucidate the functional consequences of a mutated VHL gene revealed that VHL is a key regulator of cellular hypoxia signaling. VHL controls protein levels of hypoxia-inducible factor 1- α (HIF1 α) and HIF2 α [4],

transcription factors that heterodimerize with HIF1 α and result in the transcription of proangiogenic proteins in an HIF α isoform-dependent manner [5]. Agents developed to alter the downstream consequences of VHL inactivation and inappropriate angiogenesis include bevacizumab [6], an anti-vascular endothelial growth factor receptor (VEGF) antibody, and sorafenib [7], sunitinib [8], and pazopanib [9], which are small-molecule inhibitors of vascular endothelial growth factor receptors (VEGFRs). Because all four of these agents demonstrated significant efficacy in patients with metastatic sporadic clear-cell RCC, which harbors the VHL mutation in most cases [10], they were approved by the USA Food and Drug Association for the treatment of advanced RCC.

The effect of these agents on VHL-specific lesions is not well known. We hypothesized that if the major functional consequence of VHL mutation is inappropriate angiogenesis, then blocking VEGF signaling with a potent and specific VEGFR inhibitor will alter the growth pattern of all VHL-related lesions. To test this hypothesis, we initiated a clinical trial in which we treated individuals who have genetically proven VHL with sunitinib in order to evaluate the safety and efficacy of this treatment. Because interim findings on efficacy suggested that RCCs and HBs respond differently to sunitinib,

*Correspondence to: Dr E. Jonasch, Department of Genitourinary Medical Oncology, Unit 1374, The University of Texas M. D. Anderson Cancer Center, 1155 Pressler Street, Houston, TX 77030, USA. Tel: +1-713-792-2830; Fax: +1-713-745-1625; E-mail: ejonasch@mdanderson.org

we additionally analyzed the expression and activation of various molecular markers [endothelial VEGFR, platelet-derived growth factor receptor (PDGFR), Tie2, fibroblast growth factor receptor-3 (FGFR3), and fibroblast growth factor receptor substrate-2, an intracellular signaling molecule specifically activated by FGFR3] in 20 archived tissue specimens each from sporadic RCCs and VHL-related HBs.

methods

We obtained institutional review board (IRB) approval for this prospective phase II, single-arm open-label study and obtained written informed consent from patients with genetically confirmed VHL who were undergoing surveillance for at least one measurable VHL-related lesion. Our primary objective was to evaluate the safety of sunitinib administered to those patients, and our secondary objective was to evaluate its efficacy [complete responses (CRs) + partial responses (PRs)]. Up to 28 patients were to be enrolled, but the study would be stopped early according to a continuous evaluation of toxicity.

eligibility criteria

Patients were eligible if they had no immediate need for intervention in the target or other lesions. Those with the following lesions were eligible: retinal angiomas discernible with ophthalmoscopy; cerebellar and spinal HBs at least 5 mm in longest diameter; RCCs and renal cysts with solid nodules 1–3 cm in longest diameter; and pancreatic cysts and NETs 1–3 cm in longest diameter. Patients were required to have normal organ and marrow function, as defined by serum aspartate and alanine transaminase concentrations <2.5 times the local laboratory's upper limit of normal (ULN), total serum bilirubin concentrations <1.5 times the ULN, absolute neutrophil count >1500 cells/ μ l, platelet count >100 000 cells/ μ l, hemoglobin concentration >9.0 g/dl, and serum creatinine concentration <1.5 times the ULN.

Patients with pheochromocytomas were excluded because surgical resection is considered the standard of care for treatment and because of uncertainty about how treatment with sunitinib would affect catecholamine release and blood pressure in these subjects.

clinical evaluations

Baseline and follow-up evaluations of target lesions were carried out by using computed tomography (CT) scanning or magnetic resonance imaging (MRI), as appropriate. Spiral CT scanning, involving multiphase contrast-enhanced studies of the abdomen and pelvis with thin cuts (\leq 5 mm) of the adrenals, kidneys, and pancreas, was predominantly used to follow pancreatic and renal lesions. Dynamic contrast-enhanced and diffusion-weighted MRI sequences of the brain and spinal column were used for evaluating CNS HBs.

Direct ophthalmoscopy, using fluorescein angiography with photographs, color testing, and visual field testing, was used to follow retinal lesions.

We used RECIST but modified them to uncouple target organ systems, and each organ system was evaluated separately. Summation of size was carried out separately for lesions in the kidney, pancreas, CNS (brain + spine), and retina, and these measurements were used to compare changes from baseline size.

sunitinib dosage

Patients were given oral sunitinib at a dosage of 50 mg daily for 28 days, followed by a 14-day break, for up to four cycles. Reimaging was carried out after the second and fourth cycles. Treatment was withheld if patients developed grade 3 toxic effects; it was restarted at a daily dose of 37.5 mg when the toxic effects decreased to grade 1 or lower. One further dosage

reduction, to 25 mg, was allowed if grade 3 toxic effects reoccurred, but with persistent toxicity at that dosage level, treatment was discontinued. Grade 4 non-hematologic toxicity also resulted in treatment discontinuation.

archived tissue analysis

After obtaining IRB approval, we retrieved 20 sequential formalin-fixed and paraffin-embedded specimens each of VHL-related HBs and sporadic RCCs at random from The University of Texas M. D. Anderson Cancer Center tissue bank. These samples were not derived from patients treated in the clinical trial. The specimens were analyzed at ApoCell, Inc. (Houston, TX), by using a laser-scanning cytometer (CompuCyte Corporation, Cambridge, MA), which is designed to enable fluorescence-based quantitative measurements on tissues at the single-cell level. This modality, like fluorescence-activated cell sorting analysis, provides multicolor immunofluorescence-intensity information from heterogeneous tissue specimens.

To detect biomarkers of interest, we incubated formalin-fixed tissues with CD31 (M0823; DakoCytomation, Carpinteria, CA), phosphorylated vascular endothelial growth factor receptor-2 (pVEGFR2; PC460; Calbiochem, San Diego, CA), VEGFR2 (SC-19530; Santa Cruz, Santa Cruz, CA), FGFR3 (4574; Cell Signaling), Tie2 (334208; BioLegend, San Diego, CA), phosphorylated platelet-derived growth factor receptor-beta (SC-12909-R; Santa Cruz), PDGFR (SC-339-G; Santa Cruz), and phosphorylated fibroblast growth factor receptor substrate-2 (pFRS2; 3864; Cell Signaling, Beverly, MA) antibodies, followed by species-specific secondary antibodies conjugated to fluorescent dyes (Cy5/FITC/PE; Jackson ImmunoResearch Laboratories, West Grove, PA). Each slide was placed on the computer-controlled motorized stage, and the area for scanning was visually located using the epifluorescence microscope of the cytometer, excluding normal and necrotic tissue regions. Slides were scanned using a \times 200 objective, and relative levels of fluorescence for each antigen were plotted on a scattergram. Results for biomarkers are represented as mean fluorescence intensity. Ratios of the fluorescence intensity of the phosphorylated to the total forms of VEGFR2 and PDGFR were also calculated. To detect signal in endothelial cells, relative fluorescence levels were assessed on a background of CD31 staining. For total tumor signal of antibody of interest, signal was assessed against a background of hematoxylin and eosin staining, in regions determined to be representative of tumor tissue.

VHL mutation

Data on germline mutations were acquired from the patient records. All mutational analyses were carried out by Clinical Laboratory Improvement Amendments-certified laboratories in the United States.

statistical analysis

This study was designed to include a maximum of 28 patients, but it would be stopped early if the data from a continuous evaluation of toxicity suggested that P (treatment-terminating toxicity >0.3 | data) $>90\%$. We assumed that q had a prior beta distribution of (0.3, 0.7) with a mean of 0.30 and a variance of 0.105. Thus, the study would be stopped if the number of patients with treatment-terminating toxicity in cycle 1 divided by the number of patients evaluated were 5/9, 6/10, 7/13, 8/15, 9/18, 10/21, 11/24, or 12/26.

Enrolling 14 patients would yield 83% power to detect the difference between the null hypothesis proportion of 5% response rate (PR + CR) and the alternative proportion, 30%, using an exact binomial test with a two-sided significance level of 10%, while enrolling 28 patients would yield 95% power to detect the difference between the null hypothesis proportion of 5% response rate (PR + CR) and the alternative proportion, 30%, using an

exact binomial test with a two-sided significance level of 5%. Because each individual VHL lesion is considered to have potential clinical significance in this patient population, independent analysis was carried out both on individual organ lesions and on a per-patient basis.

McNemar's chi-square test was used to assess the response outcome by RECIST in different patients. In the data analysis on individual HB and RCC lesions, repeated measurements were collected from each patient at baseline, after cycles 2 and 4, and 48 weeks after the start of treatment. Change in lesion size from baseline was assessed at those same intervals by using a linear mixed-effects model. Wilcoxon's rank sum test or Student's *t*-test was used to compare the levels of endothelial receptors in the HBs and RCCs.

results

From June 2006 to June 2009, 15 patients with VHL were recruited to participate in the trial; the study was stopped at that number of patients owing to slowing enrollment.

The patients' demographic characteristics and VHL manifestations are summarized in Table 1. VHL mutation analysis results were available for all patients (Table 1). Six patients had mutations in the elongin B–elongin C complex-binding region, and four had gross deletions or insertions leading to truncations. When mutation type was correlated to outcome, no differences were seen by major subcategory (data not shown).

All 15 patients received at least two cycles of therapy; 9 received all four. The major reasons for treatment discontinuation included patient choice (in three), clinical

progression (in two), and therapy-related toxicity (neutropenia in one). The patient choice category included patients who experienced toxic effects that did not reach grade 3 or 4 severity but who decided to discontinue treatment because of drug-related quality-of-life issues. Adverse side-effects included fatigue, diarrhea, mucositis, anemia, nausea, and hypertension (Table 2). Grade 3 toxicity included fatigue in five patients (33%), hand–foot syndrome in two (13%), nausea in two (13%), hypertension in one (7%), and neutropenia in four (26%). No grade IV or V toxic effects were encountered. The daily dosage of sunitinib was reduced in 10 patients: to 37.5 mg in 6 and to 25 mg in 4.

At least one follow-up imaging study was conducted on all patients. Table 3 shows the best responses of individual lesions according to RECIST. Of the 21 evaluable individual HB lesions, there were no PRs. In comparison, 6 of 18 RCC lesions responded with a PR, ($P = 0.014$). All five pancreatic NETs responded with stable disease. None of the seven retinal angiomas demonstrated any shrinkage on ophthalmoscopy; however, two patients with retinal angiomas complained of increased hyperemia and eye discomfort during sunitinib treatment. When change in lesion size was evaluated as a percentage by organ site per individual, RCC decreased a mean of 14.4% by the end of cycle 4, NETs a mean 12.7%, and HB 5.9% (Table 3). When size change was assessed as

Table 1. Patients' demographic characteristics ($N = 15$), types of VHL lesions, and VHL mutations

Characteristic	<i>n</i> (%)
Sex	
Male	10 (67)
Female	5 (33)
Median age (years) at treatment (range)	36 (22–57)
VHL manifestation	No. of patients with lesions (%)
Renal cell carcinomas	12 (80)
Renal cysts	11 (73)
Hemangioblastomas	11 (73)
Retinal hemangiomas	9 (60)
Pancreatic cysts	7 (47)
Pancreatic neuroendocrine tumors	7 (47)
Adrenal lesions	3 (20)
Endolymphatic sac tumor	2 (13)
Epididymal cystadenoma	1 (7)
VHL mutation	No. of patients with mutation
<i>R167W</i>	3
<i>R177X</i>	2
<i>R167P</i>	1
Deletion/truncation	4
<i>P86A</i>	1
Insertion <i>R 88-89</i>	1
<i>Y98D</i>	1
<i>X158</i>	1
<i>N131K</i>	1

VHL, von Hippel–Lindau.

Table 2. Treatment-emergent toxic effects

Toxicity	All grades	Grade 1	Grade 2	Grade 3
Fatigue	15	4	6	5
Diarrhea	13	8	4	1
Mucositis	13	7	5	1
Anemia	10	9	1	0
HFS	10	4	4	2
Rash	10	8	2	0
Nausea	9	4	3	2
Neutropenia	8	5	3	0
Dysgeusia	8	7	1	0
Sensory neuropathy	7	4	3	0
Vomiting	7	2	5	0
Skin rash	6	6	0	0
Dyspnea	6	4	2	0
Edema (H and N)	6	5	1	0
Hypertension	6	2	3	1
Pain	6	4	2	0
Headache	6	5	1	0
Anorexia	5	3	2	0
Hypophosphatemia	5	0	5	0
Epiphora	5	4	1	0
Transaminitis	4	3	1	0
Alopecia	4	4	0	0
Infection	4	2	2	0
Hyperbilirubinemia	3	2	1	0
Cough	3	3	0	0
Dysphagia	3	2	1	0
Confusion	1	0	1	0
Elevated creatinine	1	0	1	0
Epistaxis	1	1	0	0

H, head; HFS, hand foot skin reaction; N, neck.

a continuous variable, both RCCs and NETs showed significant size decrease after four cycles of sunitinib therapy.

Forty-eight-week follow-up scans were obtained for renal lesions in five patients. In these patients, who had been finished with therapy for 6 months, RCC and NETs had regrown to close to baseline measurements but no larger (Table 4).

Representative images from a patient with NETs are shown in Figure 1. This patient, who had two NETs in the head of his pancreas, initially experienced disease regression, as seen in Figure 1. At reimaging 7 months after study discontinuation, slow regrowth was seen, and the patient was retreated with sunitinib outside the bounds of the study. The lesions shrank again, and at the time this report was written, his sunitinib therapy had continued for 2.5 years with continued stability of his pancreatic lesions.

The results of laser-scanning cytometry on the archived tissue specimens from patients with VHL (20 untreated HBs and 20 untreated sporadic clear-cell RCCs) are summarized in Tables 5 and 6. VEGFR2, pVEGFR2, and phosphorylated-to-total VEGFR2 ratios were statistically significantly higher in the RCC than in the HB samples. Conversely, FGFR3 and pFRS2 levels were higher in the HBs, with a strong trend in the endothelial cells ($P = 0.059$) and significant differences in the overall tumor sample, with levels 11.45 (0.26) seen in HB versus 11.26 (0.089) in RCC ($P = 0.003$).

discussion

To the best of our knowledge, this study is the first to prospectively evaluate sunitinib therapy in patients with VHL.

Table 3. Best response of von Hippel–Lindau lesions by RECIST after sunitinib treatment

Lesion type	No. of lesions	Best response, <i>n</i> (%)		
		Partial response	Stable disease	Progressive disease
Hemangioblastoma	21	0	19 (91)	2 (9)
Renal cell carcinoma	18	6 (33)	10 (67)	2 (10)
Renal cyst	9	0	9 (100)	0
Retinal angioma	7	0	7 (100)	0
Pancreatic NETs	5	0	5 (100)	0
Pancreatic cyst	3	0	3 (100)	0

NETs, neuroendocrine tumors.

Table 4. Mean change from baseline in size of von Hippel–Lindau lesions after treatment with sunitinib

Tumor type	Mean (standard error)						
	Baseline, size (cm)	Cycle 2, size (cm)	Percent change	Cycle 4, size (cm)	Percent change	Week 48, size (cm)	Percent change
Renal cell carcinoma	2.41 (0.21)	2.04 (0.21)	-16.41 (3.9)	2.06 (0.22)	-14.42 (4.5)	2.34 (0.24)	-3.37 (5.7)
<i>P</i> value			0.0004		0.0035		0.6098
Pancreatic NET	1.89 (0.28)	1.81 (0.28)	-3.59 (3.7)	1.64 (0.28)	-12.69 (4.0)	1.89 (0.29)	-1.72 (5.2)
<i>P</i> value			0.284		0.011		0.959
Hemangioblastoma	0.81 (0.08)	0.81 (0.08)	0.65 (3.4)	0.76 (0.08)	-5.9 (5.4)	0.76 (0.09)	-6.2 (5.4)
<i>P</i> value			0.850		0.280		0.320

NET, neuroendocrine tumor.

The primary end point of the study was tolerability; 9 of the 15 patients completed all four cycles of therapy, and expected toxic effects were responsible for the necessary dosage reductions and treatment discontinuations. Three patients chose to stop early because of adverse side-effects that were not considered dose limiting. Because these patients had no acute or imminent threat from any of their VHL lesions, the balance between treatment continuation despite adverse effects and their desire to regain pretreatment quality of life was different than it is for patients dealing with metastatic disease. The secondary end point of efficacy showed significant response of RCCs, which responded better to sunitinib therapy than other VHL-related lesions did. None of the HB lesions shrank substantially, and two of them showed some progression. Pancreatic NETs shrank to a degree similar to that of RCCs, but no lesion responded with a RECIST PR. These data can be juxtaposed with the emerging data on the treatment of sporadic NETs with sunitinib, which show encouraging response rates and time to progression [11]. The evaluation of response in individual lesions is not a conventional method of reporting clinical outcomes. However, for patients with VHL, each lesion is an independent medical and surgical challenge, and a therapeutic effect on any lesion may reduce the need for surgical intervention.

A concern with the use of antiangiogenic agents is the potential for rebound to occur after treatment discontinuation. As Table 3 shows, the RCCs and pancreatic NETs had gradually regrown by the 48-week follow-up, but none of those lesions demonstrated accelerated growth kinetics.

Limitations of the current study include the conclusion of the study before maximum enrollment and the use of archival tissue that was not related to the patients in the clinical trial. Obtaining such linked tissues in this type of trial is a major challenge, as not every organ in every patient requires intervention even over prolonged periods, and as well, the goal of such studies is to minimize interventions.

The results of several small studies and individual case reports on the use of an older oral antiangiogenic agent, SU5416, in patients with VHL have been published [12–14]. Modest improvement was seen in case reports of patients with retinal involvement who were treated with SU5416 [12, 13]. A six-patient study of SU5416 reported that two patients experienced disease stabilization in CNS HBs [14]. A study carried out with intravitreally administered anti-VEGF therapy

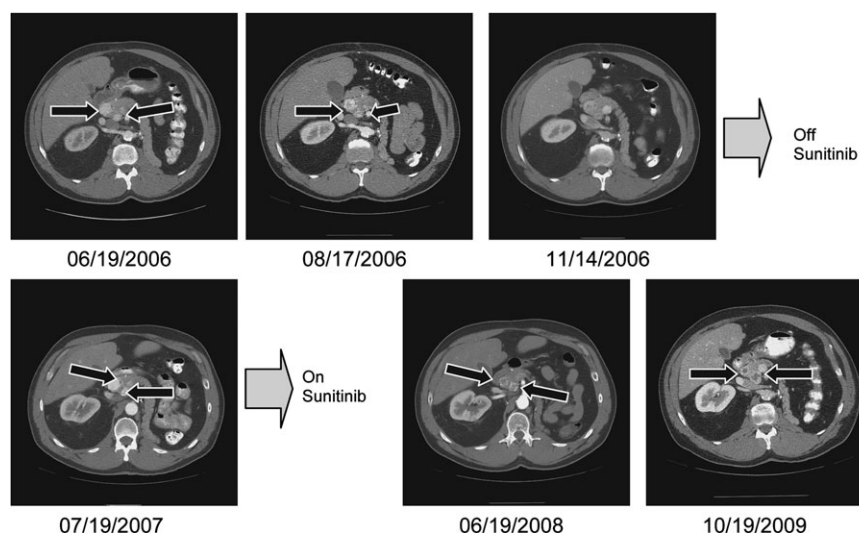


Figure 1. Pancreatic NETs after sunitinib therapy. At study initiation (06/19/2006), this patient had two pancreatic NETs (arrows) on CT scanning. Post-treatment scans (obtained 08/17/2006 and 11/14/2006) of tumors show a slight decrease in size and central necrosis. After the patient had completed the therapy regimen, scans (obtained 07/19/2007) show centripetal and centrifugal regrowth. Reinitiation of sunitinib therapy outside the bounds of the study resulted in redevelopment of central necrosis and a decrease in outside diameter (06/19/2008 and 10/19/2009). NETs, neuroendocrine tumors; CT, computed tomography.

Table 5. Endothelial receptor levels in hemangioblastomas and RCCs

Receptor	Log(hemangioblastoma)			Log(RCC)			P value (t-test)	P value (Wilcoxon's rank sum test)
	N	Mean	SD	N	Mean	SD		
pVEGFR2	20	11.268	0.498	20	11.752	0.378	0.001	0.003
VEGFR.total	20	12.977	0.478	20	13.081	0.859	0.639	0.192
pPDGFR	20	10.952	0.654	20	10.805	0.839	0.539	0.82
PDGFR.total	20	13.078	0.659	20	12.842	0.851	0.333	0.947
VEGFR.ratio	20	0.206	0.122	20	0.372	0.431	0.105	0.043
PDGFR.ratio	20	0.145	0.067	20	0.157	0.077	0.608	0.602
Tie2 in CD31-positive cells	20	12.654	0.455	20	12.63	0.817	0.909	0.883
Tie2 in tumor cells	20	11.598	0.321	20	11.614	0.303	0.866	0.947
FGFR3 in CD31-positive cells	20	12.265	0.448	20	12.29	0.961	0.914	0.495
FGFR3 in tumor cells	20	11.439	0.224	20	11.338	0.106	0.075	0.174
pFRS2 in CD31-positive cells	20	12.495	0.492	20	11.91	0.989	0.023	0.059
pFRS2 in tumor cells	20	11.452	0.258	20	11.258	0.089	0.003	0.003

RCC, renal cell carcinoma; SD, standard deviation; pVEGFR, phosphorylated vascular endothelial growth factor receptor; VEGFR, vascular endothelial growth factor receptor; pPDGFR, phosphorylated platelet-derived growth factor receptor; PDGFR, platelet-derived growth factor receptor; FGFR3, fibroblast growth factor receptor-3; pFRS2, phosphorylated fibroblast growth factor receptor substrate-2.

for a patient with retinal hemangioma yielded mixed results [15]. All these studies were limited by their small number of patients and by the type of agent used to investigate the role of antiangiogenic therapy in the management of VHL-related lesions.

The reason why organ-specific VHL-derived lesions respond differently to therapy is unclear. RCCs are true cancers, whereas HBs have no metastatic potential. Cancer-specific genetic lesions or tissue-specific endothelial heterogeneity may explain these differences in response. Data from a recent study show that endothelial cells from human RCCs strongly express VEGFR isoforms [16]. Because the putative target tissue for sunitinib is the endothelium, and in an effort to better understand this difference in tissue responsiveness, we extended our study to analyze endothelial angiogenic receptor expression

levels in archived specimens of RCCs and HBs. We hypothesized that RCCs, which had greater responsiveness to sunitinib, would also have greater VEGFR2 levels and activity and thus be more 'addicted' to this receptor than HBs are. Our results confirmed that the levels of VEGFR2 and pVEGFR2 and the ratio of phosphorylated-to-total VEGFR2 are higher in RCCs than in HBs.

Conversely, the levels of FGFR3 and pFRS2, an intracellular signaling molecule activated by FGFRs, were higher in total HB tissue than in RCC and showed a strong trend toward endothelial-specific up-regulation in HB. These findings suggest that fibroblast growth factor (FGF) pathway inhibition may affect the growth of HBs. Previous work in animal models demonstrated that up-regulation of FGF-dependent pathways can drive resistance to anti-VEGF therapy [17]. Obviously, up-

Table 6. Endothelial receptor levels in hemangioblastomas and RCCs (continued)

Receptor	Tissue	log(Hemangioblastoma)		log(RCC)		P value (t-test)	P value (Wilcoxon's rank sum test)
		Mean	SD	Mean	SD		
pVEGFR2	Endothelium	11.268	0.498	11.752	0.378	0.001	0.003
VEGFR total	Endothelium	12.977	0.478	13.081	0.859	0.639	0.192
pPDGFR	Endothelium	10.952	0.654	10.805	0.839	0.539	0.82
PDGFR total	Endothelium	13.078	0.659	12.842	0.851	0.333	0.947
VEGFR ratio	Endothelium	0.206	0.122	0.372	0.431	0.105	0.043
PDGFR ratio	Endothelium	0.145	0.067	0.157	0.077	0.608	0.602
Tie2	Endothelium	12.654	0.455	12.63	0.817	0.909	0.883
Tie2	Whole tumor	11.598	0.321	11.614	0.303	0.866	0.947
FGFR3	Endothelium	12.265	0.448	12.29	0.961	0.914	0.495
FGFR3	Whole tumor	11.439	0.224	11.338	0.106	0.0075	0.174
pFRS2	Endothelium	12.495	0.492	11.91	0.989	0.023	0.059
pFRS2	Whole tumor	11.452	0.258	11.258	0.089	0.003	0.003

RCC, renal cell carcinoma; SD, standard deviation; pVEGFR, phosphorylated vascular endothelial growth factor receptor; VEGFR, vascular endothelial growth factor receptor; pPDGFR, phosphorylated platelet-derived growth factor receptor; PDGFR, platelet-derived growth factor receptor; FGFR3, fibroblast growth factor receptor-3; pFRS2, phosphorylated fibroblast growth factor receptor substrate-2.

regulation of a receptor does not guarantee its validity as a target, and this idea requires prospective evaluation.

In conclusion, we found that sunitinib, an oral small-molecule inhibitor of VEGFR, PDGFR, Flt3, and cKit, provides a consistent response in RCCs but not in CNS HBs from patients with VHL. Endothelial VEGFR and FGFR are expressed differently in RCCs and HBs. Future studies with more potent and less toxic VEGFR inhibitors for patients with RCC lesions are warranted. Exploratory studies testing FGFR-blocking agents in patients with HB will test the hypothesis that these lesions are dependent on FGF signaling.

funding

Pfizer Pharmaceuticals Inc.

disclosure

EJ was a consultant for Pfizer. EJ and NMT received research support for clinical trials from Pfizer. All remaining authors have declared no conflicts of interest. All data acquisition, analysis, and manuscript preparation has been in the hands of the authors without industry involvement.

references

- Lonser RR, Glenn GM, Walther M et al. von Hippel-Lindau disease. *Lancet* 2003; 361: 2059–2067.
- Richard S, Campello C, Taillandier L et al. Haemangioblastoma of the central nervous system in von Hippel-Lindau disease. French VHL Study Group. *J Intern Med* 1998; 243: 547–553.
- Choyke PL, Glenn GM, Walther MM et al. von Hippel-Lindau disease: genetic, clinical, and imaging features. *Radiology* 1995; 194: 629–642.
- Maxwell PH, Wiesener MS, Chang GW et al. The tumour suppressor protein VHL targets hypoxia-inducible factors for oxygen-dependent proteolysis. *Nature* 1999; 399: 271–275.
- Raval RR, Lau KW, Tran MG et al. Contrasting properties of hypoxia-inducible factor 1 (HIF-1) and HIF-2 in von Hippel-Lindau-associated renal cell carcinoma. *Mol Cell Biol* 2005; 25: 5675–5686.
- Escudier B, Pluzanska A, Koralewski P et al. Bevacizumab plus interferon alfa-2a for treatment of metastatic renal cell carcinoma: a randomised, double-blind phase III trial. *Lancet* 2007; 370: 2103–2111.
- Escudier B, Eisen T, Stadler WM et al. Sorafenib in advanced clear-cell renal-cell carcinoma. *N Engl J Med* 2007; 356: 125–134.
- Motzer RJ, Hutson TE, Tomczak P et al. Sunitinib versus interferon alfa in metastatic renal-cell carcinoma. *N Engl J Med* 2007; 356: 115–124.
- Hutson TE, Davis ID, Machiels JP et al. Efficacy and safety of pazopanib in patients with metastatic renal cell carcinoma. *J Clin Oncol* 2010; 28: 475–480.
- Young AC, Craven RA, Cohen D et al. Analysis of VHL gene alterations and their relationship to clinical parameters in sporadic conventional renal cell carcinoma. *Clin Cancer Res* 2009; 15: 7582–7592.
- Kulke MH, Lenz HJ, Meropol NJ et al. Activity of sunitinib in patients with advanced neuroendocrine tumors. *J Clin Oncol* 2008; 26: 3403–3410.
- Girmens JF, Erginay A, Massin P et al. Treatment of von Hippel-Lindau retinal hemangioblastoma by the vascular endothelial growth factor receptor inhibitor SU5416 is more effective for associated macular edema than for hemangioblastomas. *Am J Ophthalmol* 2003; 136: 194–196.
- Aiello LP, George DJ, Cahill MT et al. Rapid and durable recovery of visual function in a patient with von hippel-lindau syndrome after systemic therapy with vascular endothelial growth factor receptor inhibitor su5416. *Ophthalmology* 2002; 109: 1745–1751.
- Madhusudan S, Deplanque G, Braybrooke JP et al. Antiangiogenic therapy for von Hippel-Lindau disease. *JAMA* 2004; 291: 943–944.
- Dahr SS, Cusick M, Rodriguez-Coleman H et al. Intravitreal anti-vascular endothelial growth factor therapy with pegaptanib for advanced von Hippel-Lindau disease of the retina. *Retina* 2007; 27: 150–158.
- Kluger HM, Siddiqui SF, Angeletti C et al. Classification of renal cell carcinoma based on expression of VEGF and VEGF receptors in both tumor cells and endothelial cells. *Lab Invest* 2008; 88: 962–972.
- Casanovas O, Hicklin DJ, Bergers G, Hanahan D. Drug resistance by evasion of antiangiogenic targeting of VEGF signaling in late-stage pancreatic islet tumors. *Cancer Cell* 2005; 8: 299–309.